

THE EFFECT OF COOLING RATE AND AUSTENITE GRAIN SIZE ON THE AUSTENITE TO FERRITE TRANSFORMATION TEMPERATURE AND DIFFERENT FERRITE MORPHOLOGIES IN MICROALLOYED STEELS

M. Esmailian

m.esmailian@irost.org

Received: June 2009

Accepted: January 2010

Advanced Materials and Renewable Energy Dept., Iranian Research Organization for Science and Technology (IROST), Tehran, Iran

Abstract: The effect of different austenite grain size and different cooling rates on the austenite to ferrite transformation temperature and different ferrite morphologies in one Nb-microalloyed (HSLA) steel has been investigated. Three different austenite grain sizes were selected and cooled at two different cooling rates for obtaining austenite to ferrite transformation temperature. Moreover, samples with specific austenite grain size have been quenched, partially, for investigation on the microstructural evolution. In order to assess the influence of austenite grain size on the ferrite transformation temperature, a temperature differences method (TDM) is established and found to be a good way for detection of austenite to ferrite, pearlite and sometimes other ferrite morphologies transformation temperatures. The results obtained in this way show that increasing of austenite grain size and cooling rate has a significant influence on decreasing of the ferrite transformation temperature. Micrographs of different ferrite morphologies show that at high temperatures, where diffusion rates are higher, grain boundary ferrite nucleates. As the temperature is lowered and the driving force for ferrite formation increases, intragranular sites inside the austenite grains become operative as nucleation sites and suppress the grain boundary ferrite growth. The results indicate that increasing the austenite grain size increases the rate and volume fraction of intragranular ferrite in two different cooling rates. Moreover, by increasing of cooling rate, the austenite to ferrite transformation temperature decreases and volume fraction of intragranular ferrite increases.

Keywords: Grain Size, Intragranular Ferrite, Cooling Rate

1. INTRODUCTION

In recent years the energy crisis has created demand for high strength and good toughness in plain carbon and High Strength Low Alloy (HSLA) steel [1, 2].

The majority of the research and development efforts have aimed at developing steels with higher strength levels and improved toughness, formability and weldability.

The investigations have resulted in recognition that with control of some parameters, resulted in certain morphologies of ferrite, the mechanical properties of steel with these ferrite structures are improved [3, 4].

The austenite to ferrite transformation, cooling rate and different ferrite morphologies are important because by controlling of these parameters, the mechanical properties of steel are improved [3, 4, 5].

It is generally agreed that the different transformation structures in continuous cooled system with decreasing temperature are as follow

[6].

- a) Grain boundary ferrite
- b) Polygonal ferrite
- c) Widmanstatten side plate ferrite
- d) Acicular ferrite
- e) Upper bainite
- f) Lower bainite and martensite

Grain boundary ferrite nucleates at the austenite grain boundary and after that Widmanstatten side plate ferrite nucleates at the grain boundary ferrite, but grows along well-defined matrix planes, while intragranular ferrite nucleates entirely within the austenite grains. Observation of the mechanical property of materials with different ferrite microstructure has shown that Widmanstatten ferrite, upper bainite or grain boundary ferrite is detrimental to toughness, whereas intragranular or acicular ferrite improves it. A comparison between acicular ferrite and bainite is shown in Fig.1.

The term acicular means shaped and pointed like a needle, but it is generally recognised that

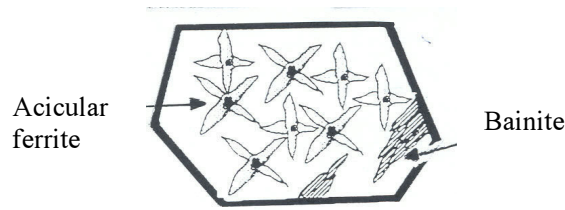


Fig.1. A comparison between different nucleation sites for bainite and acicular ferrite

acicular ferrite is three dimension species with morphology of thin, lenticular plates typically with size between 1 to 3 μm [8].

Plates of acicular ferrite cannot cross austenite grain boundary because the co-ordinated movement of atoms, implied by the shape change, cannot in general be sustained across grains having different crystallographic orientations. [8].

It is believed that propagation cleavage cracks are frequently deflected as they cross an acicular ferrite microstructure with its different orientation and this increases mechanical properties, especially toughness.

Under continuous cooling transformation (CCT) conditions, acicular ferrite formation is likely to be the final product of a series of competitive nucleation and growth reactions at the various nucleation sites [9].

A high number of oxide inclusions in weld metals and/or particles such as TiN , TiC , Nb(C, N) in plain carbon steels have strong influence on the austenite to ferrite transformation both by restricting the growth of the austenite grains as

well as by providing favourable nucleation sites for microstructural constituents such as acicular ferrite [1,2,10].

There is increasing evidence that the degree of misfit of the surface layers of inclusions/particles and bcc iron may be important in the nucleation of intragranular ferrite [11].

2. EXPERIMENTAL PROCEDURE

2.1. Steel Composition

One Nb-microalloyed steel and one austenitic stainless steel, as a standard for comparison between continuous cooling of samples, were used in the present investigation.

The compositions of Nb-microalloyed and standard steels are shown in Table 1.

Different times and temperatures for samples were used to provide austenite grain size in the range of 50-200 μm . immediately, after reheating, specimens were quenched in brine and then tempered at 500 $^{\circ}\text{C}$ for 18 hours. Table 2 shows heat treatment temperatures and times for

Table 1. Composition of Nb-microalloyed and standard samples

Elements Alloys	%C	%S	%P	%Si	%Mn	%Cr	%Ni	%Mo	%Ti	%Nb
Nb-steel	0.11	0.004	0.02	0.035	1.38	0.036	0.021	0.004	0.003	0.03
standard	0.08	0.03	0.04	1.00	2.00	16-18	10-14	2.00	-	-

Table 2. Heat treatment cycles for obtaining of different austenite grain size in alloys

Heat cycles Alloy	Peak Temp. ($^{\circ}\text{C}$)	Holding Time (min)	Average linear Intercept (μm)	A.S.T.M-G.S.N (G)
Nb-Steel	0	-	2	-
	1100	12	50	5.2
	1100	20	65	4.7
	1150	15	100	3.2
	1150	20	130	2.8
	1200	30	190	1.5
	1200	40	200	1

obtaining different grain sizes.

All the samples were sectioned adjacent to the thermocouple, polished and etched with an etchant consist of:

100 ml saturated aqueous picric acid plus 10 ml teepol

The etchant was heated to approximately 60 °C and then the specimens were immersed in etchant for 4~6 minutes.

For examination of the austenite grain size on the transformation temperature, a new method was established. In this method, the temperature of Non-transformed stainless steel specimen was compared with that of transformable steel during continuous cooling.

Paired samples, one from transformable steel and other from stainless steel as a standard, were heated to a temperature ranging between 1100 - 1200 °C to obtain approximately 50, 100 or 200 μm austenite grain size for the specimens. After heating in a inert atmosphere (N₂ gas) and holding for 12 to 40 minutes in the furnace, the samples were taken out and cooled in air by two cooling rate. The temperature and time were recorded by a data logger for pair of standard and specimen. A schematic of TDM method is illustrated in Fig.2.

The temperature difference (dt) between transformable specimen (Nb-microalloyed steels) and a standard (stainless steel sample) was drawn as a function of temperature, while the specimen and standard steels were subjected to a controlled temperature programme. Exothermic heating of

specimens, compare to the constant heating of standard, resulted in the changing of slopes from which the start and end of transformation can be detected.

The temperature-time were recorded during cooling from the austenitic temperature to the finishing temperature was corrected to be equivalent to compensate isothermal holding. This was done using the following equation [12].

$$t_{equiv} = \sum t_i \exp(-Q/RT_i) / \exp(-Q/RT) \quad (1)$$

Where Q is activation energy for diffusion of carbon in austenite (171.5KJ/mol) R is gas constant and t and T are time and temperature [13].

In order to understand the development of microstructure, specimens were heated using the same cycles in previous examination to obtain 50, 100 and 200 μm austenite grain size. On the base of transformation temperatures which had been found by Temperature Difference Method (TDM), the specimens were quenched by 20 °C intervals in the brine from the start to the end of transformation temperature by two cooling rate (5.5 °C/s and 12.5 °C/s). The samples were then sectioned and investigated by optical and electron microscopy.

Point counting instrument assembled to optical microscope was used to determine the volume fraction of each phase.

Scanning Electron Microscopy (SEM) was used to provide more reliable evidence of the

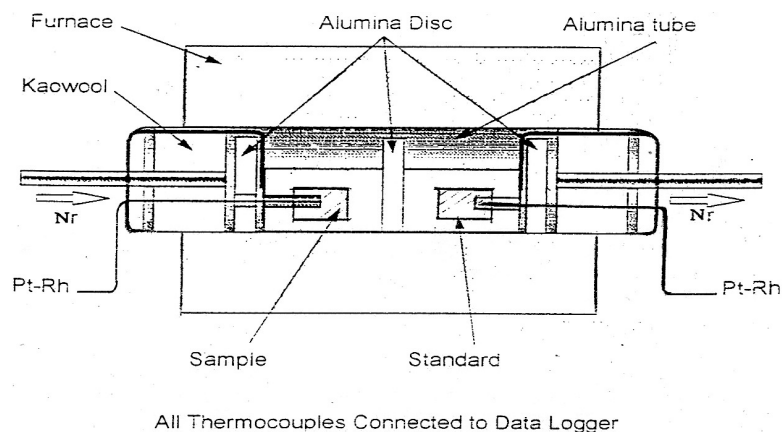


Fig. 2. A schematic illustration of TDM instrument for obtaining transformation temperatures

features found with the aid of optical microscopy. Some particles in Nb-microalloyed steel were quantitatively analysed using Energy Dispersive Spectroscopy (EDS) and counting time of 100.

3. RESULTS AND DISCUSSION

3.1. Austenite Transformation Temperature Behaviour During Cooling

For evaluation of start, final and intermediate ferrite morphologies, Dt-t diagram draw (Fig. 3) and shows that ferrite start temperature transformation T_s (point a) for sample with 50 μm austenite grain size and 5.5 $^{\circ}\text{C/s}$ cooling rate is 660 $^{\circ}\text{C}$. Subsequently, Widmanstatten (Ws) and acicular ferrite (As) (point b) nucleate.

Moreover, the diagram shows that the end of transformation for sample with 50 μm austenite grain size occurs at 580 $^{\circ}\text{C}$ (point c).

Moreover, diagrams show that by increasing austenite grain size T_s , A_s and end of transformation (T_f) decreases to 620 $^{\circ}\text{C}$ for 100micron and 610 $^{\circ}\text{C}$ for 200 micron austenite grain size samples subsequently (Figs. 4 A,B). Furthermore a comparison between two samples with the same austenite grain size and different cooling rate (Fig. 3A and Fig. 4C) shows that by increasing of cooling rate from 5.5 to 12.5 $^{\circ}\text{C/s}$, the T_s , A_s and T_f decreases 20 $^{\circ}\text{C}$ as well.

3. 2. Kinetics of Grain Boundary Ferrite

Fig. 5 shows the relationship between time and

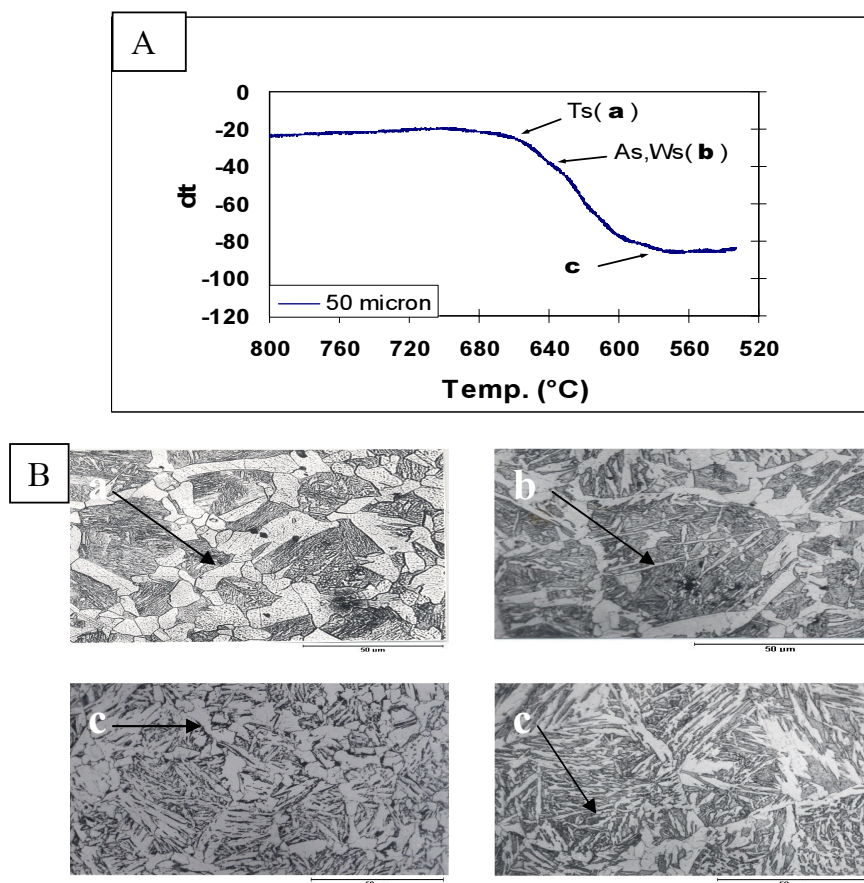


Fig. 3. Illustration of grain boundary ferrite and intragranular start temperatures, end of reaction and related microstructures

- Diagram A: T_s (ferrite start temperature), A_s, W_s (Acicular and Widmanstatten start temperature), C (End of ferrite transformation)
- B: Photograph of related Microstructures: a (Grain boundary ferrite), b (Acicular ferrite), c (Pearlite start)

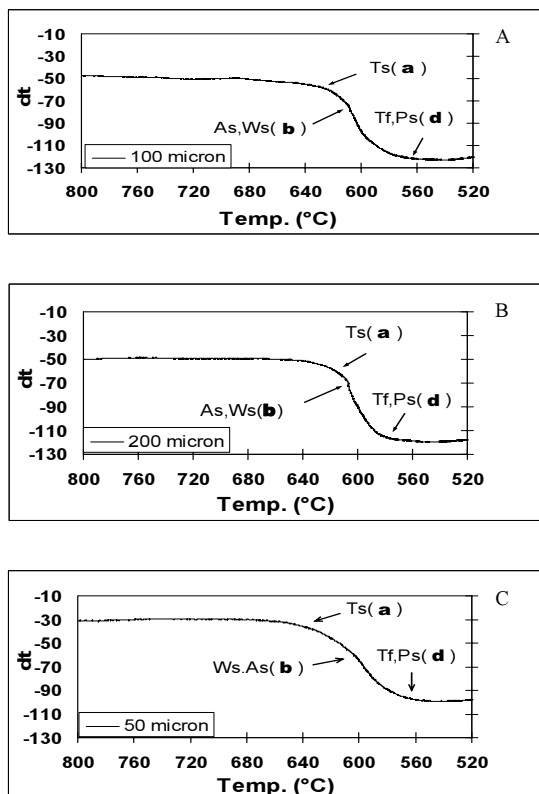


Fig. 4. Illustration of grain boundary ferrite and intragranular start temperatures and end of reaction for:
 A: Sample with 100 micron austenite grain size and 5.5 $^{\circ}C/s$ cooling rate
 B: Sample with 200 micron austenite grain size and 5.5 $^{\circ}C/s$ cooling rate
 C: Sample with 50 micron austenite grain size and 12.5 $^{\circ}C/s$ cooling rate

volume fraction of grain boundary ferrite versus three different austenite grain sizes by 5.5 $^{\circ}C/s$ cooling rate.

Kinetics of grain boundary reaction in this alloy shows that nucleation of intragranular ferrite inside the austenite grains prevents from nucleation of idiomorph ferrite and affects the kinetics behaviour of reaction. Moreover, diagram shows that by increasing of austenite grain to 200 μm a huge decrease in volume fraction of grain boundary ferrite can be seen.

Reduction in transformation temperature should resulted in less time and diffusivity for the growth of grain boundary ferrite and hence reduction in primary ferrite volume fraction and consequently in an increase of the acicular ferrite content [13].

In this alloy a considerable decrease from 35 to 10% in volume fraction of grain boundary ferrite shows that, increasing of austenite grain size is more effective for nucleation of intragranular ferrite morphology. Moreover results show that reaction time for completion of grain boundary ferrite decreases with increase of austenite grain size.

3.3. Kinetics of Intragranular Ferrite

The results show in Fig. 6 and Fig. 7 indicate that increasing the austenite grain size increases the rate of reaction and volume fraction of



Fig. 5. Relationship between volume fraction of grain boundary ferrite and time of reaction

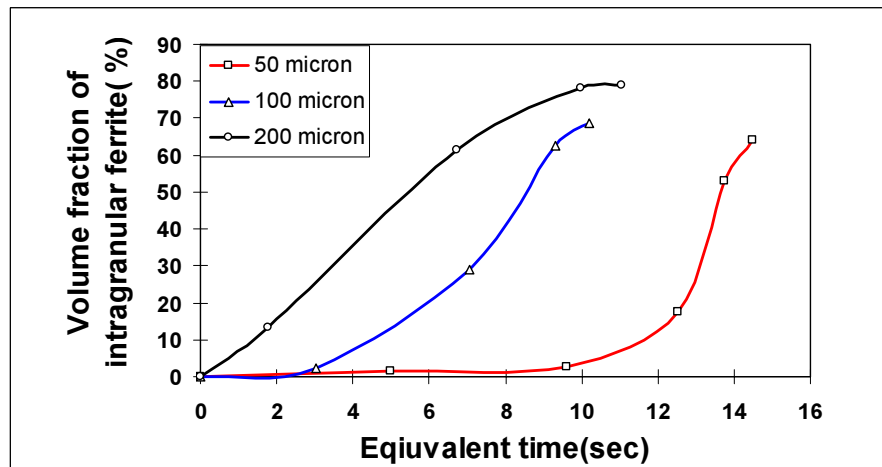


Fig. 6. Relationship between volume fraction of intragranular ferrite and time of reaction in samples by 5.5°C/s cooling rate

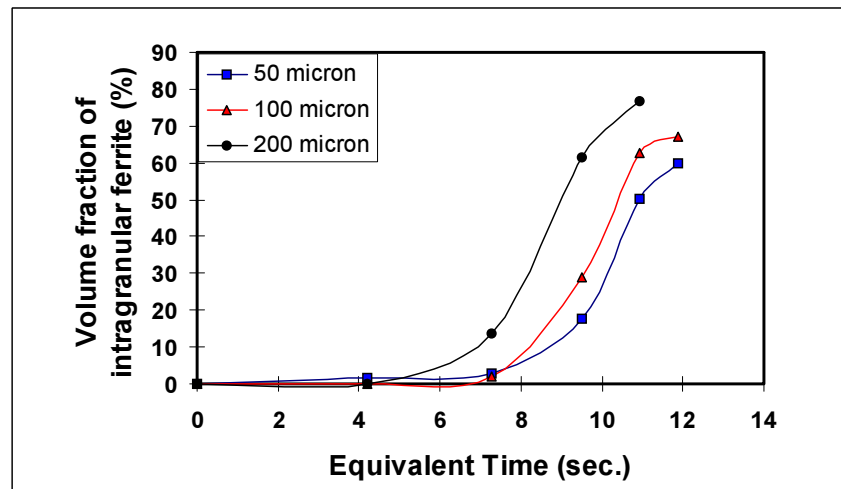


Fig. 7. Relationship between volume fraction of intragranular ferrite and time of reaction in samples by 12.5°C/s cooling rate

intragranular ferrite in two different cooling rates.

All curves show exponential form and an incubation time for reaction can be seen for all different austenite grain size, but with increasing the austenite grain size this time decreases. Moreover, diagrams show that with increasing the austenite grain size, the time for completion of reaction decreases.

In the case of acicular ferrite, it seems that increase in austenite grain size causes decrease of transformation temperature and hence increases the number of particles which can be removed from solution. In the next step, this new particles (NbC, TiN) inside the austenite grains become

operative by providing favourable nucleation sites for acicular or intragranular ferrite formation and results clearly show that by increasing the austenite grain size, the volume fraction of acicular ferrite increases.

Thewlis et al. [9] in their work reported that acicular ferrite is not a single transformation product, but forms as a result of succession of nucleation and growth with shear reaction. The rate of reaction in the first step is very slow as compared to that in final step, which is very fast, and microstructural observations show close agreement with this view.

A comparison between two different cooling rates show that increasing of cooling rate effects

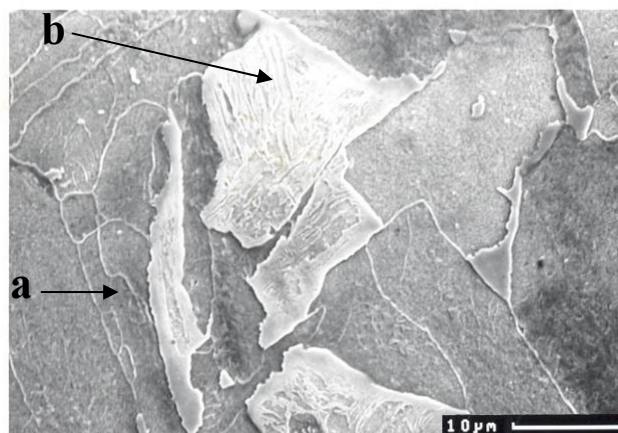


Fig. 8. Illustration of progress of intragranular ferrite nucleation inside the austenite grains by SEM photograph during the cooling

on the incubation time and by decreasing of cooling rate the incubation time decreases in high austenite grain size samples.

The SEM results indicate that intragranular ferrite inside the alloy exhibits different forms. The grain boundary ferrite has plate shape, while the intragranular ferrite becomes more degenerated plate-like, lens-like or rosette shaped (Fig.8,a). Moreover, the SEM results indicate that nucleation of intragranular ferrite progresses with nucleation and growth over almost entire range of transformation inside the austenite grains by different rate of nucleation (Fig.8,b).

4. CONCLUSIONS

Temperature Difference Method (TDM) is a good technique which clearly can detect the start and end of ferrite transformation and sometimes other ferrite morphologies such as acicular ferrite and pearlite reaction.

It is very desirable to produce large austenite grain size in the Nb - microalloyed steels. This promotes high volume fraction of desirable acicular ferrite, provided other ferrite morphologies do not form.

A shift from grain boundary ferrite to acicular microstructure occurs parallel to the degree of supercooling in sample with 50, 100 and 200μm austenite grain size in this alloy.

Nucleation of fine intragranular ferrite (acicular ferrite) is aided by inclusions when

factors such as austenite grain size, cooling rate and sympathetic nucleation combine to produce conditions within the prior austenite grains.

Increasing of cooling rate increases incubation time, especially for large austenite grain size, and decreases time for completion of reaction and increases nucleation of acicular ferrite.

REFERENCES

1. Deardo, A.J., J. M. Gray., and Meyer, L., *Fundamental metallurgy of Niobium in steel*, ed. H. Stuart, (AIME), USA, 1981, 685
2. Crooks, M.J., A. J. Garratt-Reed, J. B. Vander Sande and Owen, W.S., *Precipitation and recrystallization in some Vanadium and Vanadium-Niobium microalloyed.*, *Metallurgical Transaction A*, 1981, 12A.; 1999-2013.
3. Galibois, A., M.R.Krishnadev., and Dube, A., *Control of grain size and substructure in plain carbon and high strength low alloy (HSLA) steels.* *Metallurgical Transaction A*, 1979, 10 A, 985-995
4. Harrison, P.T., and Farrar, R. A., *Influence of Oxygen rich inclusions on the austenite ferrite phase transformation in HSLA steel weld metals.*, *Journal of Materials Science*, 1981, 16, 2218-2226
5. Tomita, Y., *Effect of continuous cooling transformation structure on mechanical properties of 0.4C-Cr-Mo-Ni steel.*, *Journal of Material Science*, 1994, 29, 1612-1616

6. Compendium of Weld Metal Microstructures and Properties, ed. The Welding Institute, Cambridge, 1985, pp. 98-100
7. Babu, S. S. and Bhadeshia, H.K.D.H., *Transformation from bainite to acicular ferrite in reheated Fe-Cr-C weld deposits.*, *Materials Science and Technology*, 1990, 6, 1005-1019
8. Honeycomb, R.W.K., and R.W.Kerr, *Steels, microstructure and properties*, ed. Edward Arnold, London, 1981, pp. 78-79
9. Thewlis, G., J. A. Whiteman and Senogles, D. J., *Dynamics of austenite to ferrite phase transformation in ferrous weld metals.*, *Materials Science and Technology*, 1997, 13(March), 267-274
10. Grong, O., and Matlock, D. K., *Microstructural development in mild and low alloy steel weld metals.*, *International Metals Reviews*, 1986, 31(1), 27-47
11. Mills, A.R., G. Thewlis., and Whiteman, J. A., *Materials Science Technology*, 1987, 3(1), 1051-1061
12. Sellars, C.M., and Whiteman, J. A., *Recrystallization and grain growth in hot rolling.* *Metal Science*, 1979, March-April, 187-194
13. Manohar, P.A., T. Chandra and Killmore, C. R., *Continuous cooling transformation behaviour of microalloyed steels containing Ti, Nb, Mn and Mo.*, *ISIJ International*, 1996, 36(12), 1486-1493